Mixed clonal-aggregative multicellularity entrained by extreme salinity fluctuations in a close relative of animals

Núria Ros-Rocher[1*], Josean Reyes-Rivera[2*], Yeganeh Foroughijabbari[1], Chantal Combredet[1], Ben T. Larson[2,3], Maxwell C. Coyle[2], Erik A.T. Houtepen[4], Mark J. A. Vermeij[4,5], Nicole King[2], Thibaut Brunet[1+]

[1]Institut Pasteur, Université Paris-Cité, CNRS UMR3691, Evolutionary Cell Biology and Evolution of Morphogenesis Unit, 25-28 Rue du Dr. Roux, 75015 Paris, France

[2]Howard Hughes Medical Institute and the Department of Molecular and Cell Biology, University of California, Berkeley, Berkeley, CA, USA

[3]Present address: Department of Biochemistry and Biophysics, University of California, San Francisco, San Francisco, CA, USA

[4]Caribbean Research and Management of Biodiversity foundation (CARMABI), Piscaderabaai z/n Willemstad, Curaçao

[5]Department of Freshwater and Marine Ecology, Institute for Biodiversity and Ecosystem Dynamics, University of Amsterdam, Amsterdam, 1012 WP, The Netherlands

*Contributed equally

+Lead contact

Correspondence: T.B.: thibaut.brunet@pasteur.fr

Abstract

Multicellularity evolved multiple times independently during eukaryotic diversification. Two distinct mechanisms underpin multicellularity: clonal development (serial cell division of a single precursor cell) and aggregation (in which independent cells assemble into a multicellular entity). Clonal and aggregative development are traditionally considered to be mutually exclusive and to result from independent acquisitions of multicellularity. Here, we show that the choanoflagellate *Choanoeca flexa*, a close relative of animals that forms contractile monolayers of cells (or "sheet colonies"), develops by an unconventional intermediate mechanism that we name "clonal-aggregative multicellularity". We find that *C. flexa* sheets can form through purely clonal processes, purely aggregative processes, or a combination of both, depending on experimental conditions. To assess the ecological relevance of these findings, we characterize the natural context of multicellular development in the native environment of *C. flexa* on the island of Curaçao. We show that the *C. flexa* life cycle is environmentally regulated by extreme salinity fluctuations in splash pools undergoing cycles of evaporation and refilling. Upon desiccation, *C. flexa* colonies dissociate into drought-resistant quiescent cells, which resume activity and reform multicellular sheets after rehydration. We hypothesize that clonal-aggregative development reflects selection for fast transitions into and out of multicellularity in the ephemeral context of coastal splash pools. Our findings underscore the potential of the exploration of biodiversity for revealing new fundamental biological phenomena and expand the known option space for both multicellular development and for the origin of animal multicellularity.

Introduction

The transition to multicellularity was a key event in animal evolution. Multicellularity has evolved independently over 45 times across eukaryotes (*1*) and can develop by two main mechanisms canonically depicted as mutually exclusive (*2–4*): clonal development or aggregative development (also referred to as “staying together” versus “coming together”, respectively (*5*)). During clonal development, a single founder cell undergoes serial cell divisions without separation of sister cells, resulting in a genetically identical multicellular structure. In contrast, aggregative development refers to the formation of multicellular entities by grouping and coalescence of independent cells. Contrary to clonal development, aggregation allows genetically distinct cell populations to combine into chimeric multicellular structures (*6*). The potentially low degree of genetic relatedness within aggregates can result in evolutionary conflict (*e.g.* vulnerability to "cheaters"; see glossary) and has been argued to limit the potential for aggregation to give rise to complex multicellularity, alongside the fact that aggregative multicellularity tends to be transient and facultative (*7–11*). Indeed, all five eukaryotic lineages with "complex multicellularity” (*i.e.* controlled three-dimensional morphogenesis and spatial cell differentiation), including animals, fungi, and land plants, develop clonally rather than by aggregation (*3*, *8*).

Despite the apparent evolutionary limitations of aggregative multicellularity, one remarkable feature of aggregation is the speed with which aggregative organisms can complete multicellular development from a unicellular state (often over a few hours (*6*, *6*, *12*)). Aggregative multicellularity is often a stress response to environmental changes such as nutrient depletion (*13*, *14*) or the presence of predators (*15–17*). In such situations, aggregation allows for rapid establishment of a multicellular structure that confers some selective advantage (*e.g.* increased size, shielding of inner cells by a protective cell layer, or elevation from the substrate via formation of a stalk). This mechanism is faster than clonal division, and might be especially beneficial when cell proliferation (and therefore clonal development) is infeasible (*6*, *13*, *17*). Thus, it has been argued that aggregation can be ecologically more advantageous than clonal development in fast-fluctuating environments, including conditions of acute stress (as an “emergency response”) (*6*, *10*, *18*).

Efforts to reconstruct the evolution of multicellularity in the stem lineage of animals have benefited from the study of their closest living relatives (the unicellular and facultatively multicellular holozoans (see glossary)) and notably of their sister group: the choanoflagellates (**Figure 1A**) (*19–22*). Choanoflagellates are bacterivorous aquatic microeukaryotes bearing

an apical flagellum surrounded by a collar of interconnected actin-filled microvilli (**Figure 1B-C**) (*23*). Flagellar beating causes a water flow that carries bacterial prey toward the collar, where the bacteria are trapped and ultimately phagocytosed. Choanoflagellates can differentiate into diverse cell types, and can develop into facultative multicellular forms in many species (*3*, *23–26*). As in animals, multicellular development is clonal in all choanoflagellate species investigated so far, which contrasts with the occurrence of aggregative multicellularity in more distantly related lineages, such as filastereans (*27–30*) and dictyostelid amoebae (*13*, *31*). These observations have inspired the hypothesis that animals evolved from organisms with a simple form of clonal multicellularity, akin to that observed in certain modern choanoflagellates (*3*, *32–34*).

Here, we describe an unusual type of multicellular development in the colonial choanoflagellate *Choanoeca flexa* (*35*), which challenges previous generalities about choanoflagellates. We report that *C. flexa* colonies develop by a combination of clonal and aggregative development, which we refer to as 'clonal-aggregative multicellularity'. This mixed mode of development has never been formally described in choanoflagellates or other protists to our knowledge and nuances the textbook dichotomy between clonal and aggregative modes of multicellular development. We show that *C. flexa* clonal-aggregative development occurs in the context of a life cycle entrained by salinity fluctuations encountered in their natural habitat: splash pools that undergo cycles of evaporation and refilling on the timescale of a few days. We propose that this extreme, fast-fluctuating environment might have contributed to selecting for this unusual mode of multicellularity. Our observations establish *C. flexa* as a new model for the ecological context and developmental mechanisms of facultative multicellularity across close relatives of animals and expand the range of possible scenarios for the emergence of animal multicellularity.

Results

C. flexa was discovered in 2018 in splash pools (see glossary) on the rocky coast of the Caribbean island of Curaçao in the form of curved multicellular "sheet" colonies (**Figure 1A-D**) (*35*). Cells within *C. flexa* colonies are held together through direct collar-collar interactions, forming a concave monolayer of cells with aligned apico-basal polarity (**Figure 1B-D**) (*35*, *36*). *C. flexa* sheets display collective contractility under the control of environmental cues (including light-to-dark transitions), inverting their curvature and switching from a feeding state (relaxed form, flagella-in; **Figure 1B**) to a swimming state (contracted form, flagella-out;

117 **Figure 1D**) (*35*, *37*). In an earlier study, we established stable cultures of *C. flexa* sheets from
118 a single isolated cell, indicating that sheets can arise from individual cells (*35*). Nevertheless,
119 the mechanisms of *C. flexa* multicellular development remained unexplored.
120

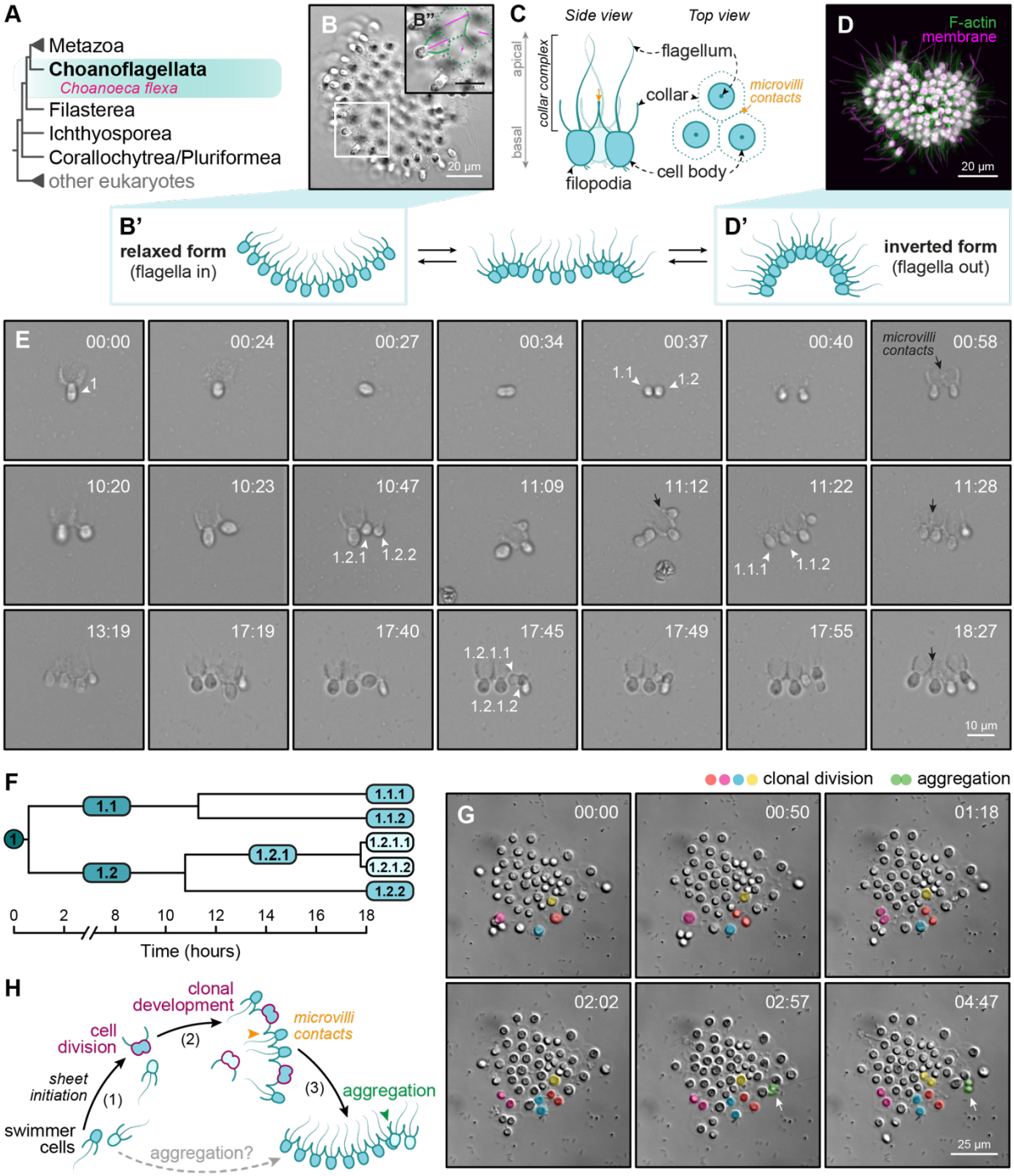

121
122 *(Figure 1 legend on the next page)*

Figure 1. *Choanoeca flexa* can develop clonally but also displays aggregative features. (A) Choanoflagellates (turquoise) are the sister group to animals (Metazoa). The phylogenetic relationships depicted are based on several recent phylogenomic studies (*3*, *25*, *27*, *35*, *38–41*). Uncertain positions are represented with polytomies. (B) Brightfield image of a *C. flexa* multicellular colony ("sheet") in its relaxed conformation (B'). B", white square: zoom-in showing flagella (magenta pseudocolor) and direct cell-cell contacts between collars (green pseudocolor). Scale bar in B'': 10 µm. (C) Diagnostic morphological features of a choanoflagellate cell. *C. flexa* cells within a sheet are linked by their collars (orange arrow). (D) 3D reconstruction of an Airyscan Z-stack of a fixed sheet exhibiting an inverted conformation (D'), with cell bodies stained with a membrane/cytoplasmic dye (FM™ 1-43FX, magenta, which distributes to the membrane and cytoplasm of cells following fixation), and microvilli stained with a filamentous actin (F-actin) dye (phalloidin Alexa 488, green). (E) Stills from a brightfield timelapse movie of clonal *C. flexa* sheet development by serial cell division from a single *C. flexa* swimmer cell (white arrowhead). After each division, the sister cells remain adhered to each other by direct cell-cell contacts between collars (black arrow). Note that cells retract their flagellum during division. Time scale hh:mm. (F) Cell lineage tracing as a function of time in E shows that cells divide asynchronously during colony formation, taking ~8-10 hours between each round of division. (G) Stills from a brightfield timelapse movie depicting a medium-sized *C. flexa* sheet (flagella-in conformation) that expands in cell number both by cell division (pseudocoloring in orange, pink, blue and yellow) and by cellular aggregation (white arrow, pseudocoloring in green). Time scale hh:mm. (H) Schematics of *C. flexa* mixed clonal-aggregative multicellularity development observed under laboratory culture conditions: (1) unicellular flagellate (swimmer) cells can divide clonally to initiate a colony; in turn, colonies can increase in cell number by (2) clonal division and (3) cellular aggregation (green arrowhead). In all cases, sister cells resulting from cell division or independent cells attaching to colonies by cellular aggregation adhere to each other through direct cell-cell contacts in their collar (orange arrowhead). The hypothesis that *C. flexa* sheets might be able to develop purely by aggregation is tested in Figure 2. Figure related to **Figure S1** and **movies S1-S3**.

C. flexa sheets can develop clonally but are also able to expand by aggregation

To understand *C. flexa* colony development, we first isolated and monitored single cells from mechanically disassembled sheets by time-lapse microscopy. In this context, we observed clonal development of sheets by serial cell division (**Figure 1E-F; movie S1**). After cell division, sister cells remained attached to each other by intermicrovillar contact. Cells continued to divide asynchronously (every ~8-10 hours), resulting in a monolayer of polarized cells with the signature curved morphology of *C. flexa* sheets (**Figure 1E-F; movie S1**). These observations show that small *C. flexa* sheets (up to 7 cells) can develop clonally from a single cell. To test whether clonal development can contribute to the further growth of *C. flexa* colonies, we monitored small- and medium-sized colonies (between 6 and 46 cells) by time-lapse microscopy and regularly observed clonal expansion by cell division both at the core and periphery of the sheets (**Figures 1G and S1; movies S2-S3**). However, unexpectedly, we also captured instances of free-swimming single cells and doublets meeting colonies, attaching to their periphery, re-orienting their apico-basal polarity to align with neighboring cells, and seemingly integrating into the sheet (**Figures 1G and S1; movies S2-S3**). Taken together, these results show that *C. flexa* colonies can form clonally but can also expand by

162 aggregation. This motivated us to test whether *C. flexa* could also acquire multicellularity
163 purely by aggregation (**Figure 1H**).
164
165 **Aggregation is sufficient for multicellular development in *C. flexa***
166
167 To test whether *C. flexa* colonies can form by aggregation, we mechanically disassembled
168 colonies into free-swimming single cells and performed live imaging of the dissociated cells
169 (**Figure 2A; movie S4**). We found that *C. flexa* single cells aggregated within minutes into
170 irregular masses of cells that continued incorporating additional cells and underwent repeated
171 fusion into larger groups (a process known as agglomeration (*42*); **Figure 2A; movie S4**). To
172 determine the fate of these aggregates, we labeled two populations of dissociated single cells
173 with different fluorophores. Mixing both populations was followed by aggregation of cells of
174 both colors within minutes (**Figure 2B; movie S5**). After 24 hours, we observed chimeric
175 colonies displaying the polarized cup-shaped morphology typical of canonical *C. flexa* sheets
176 and comprising cells of both colors (**Figures 2C and S2A; movies S6-S8**), indicating that
177 they had developed by aggregation. To better understand the dynamics of aggregative
178 development, we fixed aggregates at different stages and imaged them by Airyscan confocal
179 microscopy. We found that early aggregates (fixed up to 6 hours post-dissociation (6 hpd))
180 displayed a variable and irregular morphology with cells frequently showing unaligned apico-
181 basal polarity, likely resulting from collision and attachment of cells in diverse random
182 orientations (**Figures 2D and S2B; movies S9-S12**). Colonies observed 24 hpd, on the other
183 hand, consistently showed *bona fide C. flexa* sheet morphology with regularly aligned cells
184 (**Figures 2D and S2B; movie S13**), suggesting that early irregular aggregates had by then
185 completed their maturation into canonical sheets. At that stage, colonies comprised about 50
186 cells on average and as many as 120 cells (**Figure 2E**). This size further supported the idea
187 that these sheets could not have formed exclusively by clonal development within 24 hours,
188 given the cell cycle duration in *C. flexa* (at least 8 hours, which could result in sheets
189 comprising at most 16 cells assuming maximal and synchronized proliferation; see **Figure**
190 **1F**).

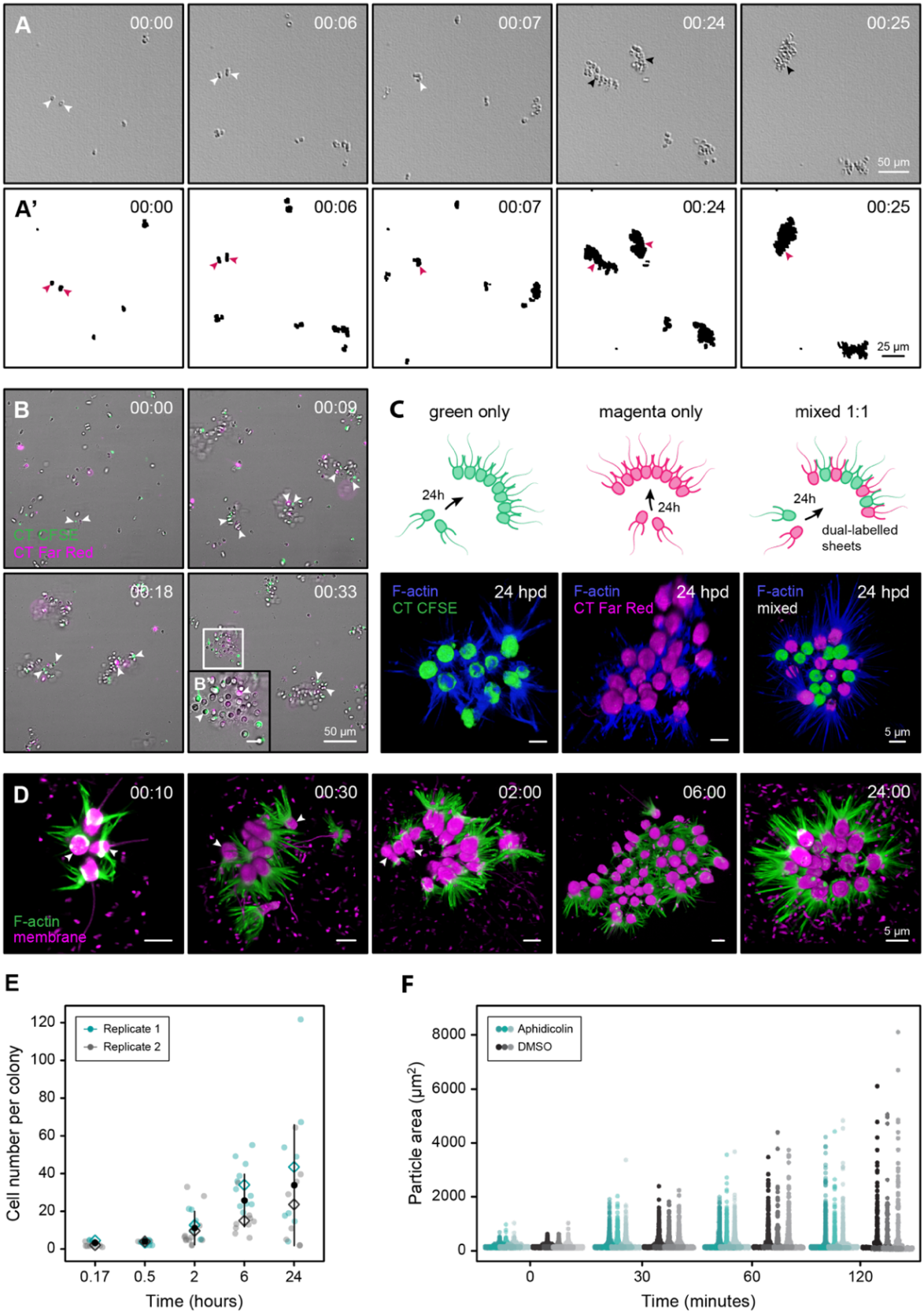

(Figure 2 legend on the next page)

Figure 2. Multicellularity in *C. flexa* can be established purely by aggregation. (A) Stills from a brightfield timelapse movie showing that dissociated single cells (white arrowheads) quickly re-formed colonies by cellular aggregation. Note that two colonies can fuse together by agglomeration (black arrowheads). (A') Binary image mask of stills in A. Time scale hh:mm. (B) Stills from a timelapse movie showing that two dissociated single cell populations labelled with either Cell Trace CFSE (green) or Cell Trace Far Red (magenta) aggregated into dual-labelled chimeric groups of cells (white arrowheads). Time scale hh:mm. B', white square: zoom-in showing a dual-labelled colony. Scale bar: 10 µm. (C) (Upper panels) Dissociated single flagellate cells labelled with Cell Trace CFSE (left, green) or Cell Trace Far Red (middle, magenta) form single-labelled colonies 24 hours post-dissociation (hpd). When both single celled populations are mixed in a 1:1 ratio, they form dual-labelled colonies (right). (Lower panels) 3D reconstructions of Airyscan Z-stacks of sheets formed by aggregation from dissociated single cells labelled as depicted above and fixed 24 hpd, with additional filamentous actin (F-actin) staining (phalloidin Alexa 405, blue). (D) 3D reconstructions of Airyscan microscopy images of single cells fixed after 10 minutes (n=12), 30 minutes (n=12), 2 hours (n=19), 6 hours (n=20) and 24 hours (n=16) post-dissociation stained for membrane/cytoplasm (FM™ 4-64FX, magenta) and F-actin (phalloidin Alexa 488, green). Note that cells frequently show unaligned apico-basal polarity and diverse cell orientations at early timepoints (white arrowheads). Time scale hh:mm. (E) Quantification of cell number per colony during aggregation (from the experiment in D) in two independent biological replicates. Black circles: mean. Error bars: standard deviation. Diamonds: mean values of independent biological replicates. (F) Quantification of particle area during an aggregation time course of dissociated single cells pre-treated with 17 µg/mL aphidicolin overnight in three independent biological replicates. DMSO: negative control. Figure related to **Figures S2-S3** and **movies S4-S13**.

Indeed, treatment with the cell cycle inhibitor aphidicolin abolished cell proliferation (**Figure S3**) but did not prevent colony formation from dissociated cells (**Figure 2F**), confirming that aggregation was sufficient for *C. flexa* multicellular development.

Our observation of aggregative development in *C. flexa* contrasts with earlier observations in other species of multicellular choanoflagellates, which had so far been found to develop strictly clonally (*3*, *23*, *24*). Given that other protists often deploy aggregative development as an "emergency response" to fluctuating environments (*4*, *14*), while clonal development is thought to more frequently result in stable structures capable of feeding and cell proliferation, we were curious about the natural conditions of *C. flexa* mixed clonal-aggregative development. Thus, we set out to investigate the natural ecological context of *C. flexa* multicellular development.

Multicellular *C. flexa* sheets occur in a restricted salinity range in their natural environment

C. flexa was originally discovered in its multicellular form on the Caribbean island of Curaçao (*35*), a semi-arid tropical island that experiences dry and rainy seasons (**Figure 3A**) (*43*). Unlike other multicellular choanoflagellate species (*20*, *44*), *C. flexa* has been repeatedly re-isolated in the wild since its discovery in 2018 and can thus be studied in its natural environment. *C. flexa* sheets are found in splash pools on the wind-exposed northern part of

the island (**Figures 3A-B and S4A-B**) that undergo natural cycles of desiccation and refilling (*45*, *46*). Water-filled splash pools experience gradual evaporation, leading to increasing salinity and, occasionally, complete desiccation (**Figure 3C**). Splash pools refill from crashing waves, splash, or rain, restoring lower salinity levels (**Figures 3C and S4B; movie S14**). Splash pools are, consequently, ephemeral habitats in which organisms often experience extreme and recurrent hypersaline and hyperosmotic stress (*46–49*). Thus, we investigated how this highly fluctuating environment might influence the life history and multicellular development of *C. flexa*.

We focused our studies on Shete Boka (meaning "seven bays" in Papiamento) National Park, where *C. flexa* is reliably found (**Figure 3A**). We surveyed the distribution of *C. flexa* in 150 splash pools and measured splash pool salinity in two different field expeditions: Exped-A and Exped-B (**Figure 3D**). During Exped-A, we randomly sampled 79 splash pools (numbered Sp1 to Sp79) along about 2 kilometers of coastline in Shete Boka (**Figure 3D**; see methods). While seawater collected from the neighboring inlets or *bokas* had a stable salinity of 40 parts per thousand (ppt), splash pool salinity ranged from below average seawater salinity (25 ppt) to saturation (≥ 280 ppt) (**Figures 3E and S4C**).

In 10 out of 79 splash pools, we found sheets that exhibited the stereotypical *C. flexa* cup-shaped morphology and inversion behavior in response to light-to-dark transitions (*35*) (**Figures 3F and S5A-C; movie S15**). 18S ribosomal DNA sequencing of manually isolated sheets confirmed their identification as *C. flexa* (**Figure S5D; supplementary files S1-S4**). Interestingly, although the salinity of surveyed splash pools ranged from 0.6-fold to 7-fold of that measured in seawater from the neighboring *bokas*, *C. flexa* sheets were only found in splash pools with <2-fold seawater salinity (<73 ppt; **Figures 3E and S4C**). To independently test whether the presence of multicellular *C. flexa* was constrained by an upper bound of salinity, we employed a different sampling strategy during a second expedition (Exped-B) in which we exhaustively sampled all splash pools within a 4-meter by 10-meter quadrant (n=71, numbered Sp1 to Sp71; **Figure 3D**; see methods). We found sheets in 14 out of 71 splash pools, with a 94 ppt salinity upper bound for sheet occurrence (**Figures 3E and S4C**). Across both expeditions, *C. flexa* sheets were found in splash pools with an average salinity of 61.42 ± 17.54 ppt, 1.56-fold higher than natural seawater from the *bokas* (**Figures 3E and S4C**) and significantly lower than the salinity of sampled splash pools that did not contain sheets (155.1 ± 107.2 ppt; p=3.1e-04 by the Mann-Whitney U test). We never observed sheets in splash pool water with a salinity above 94 ppt (2.35-fold seawater salinity; **Figures 3E and S4C**).

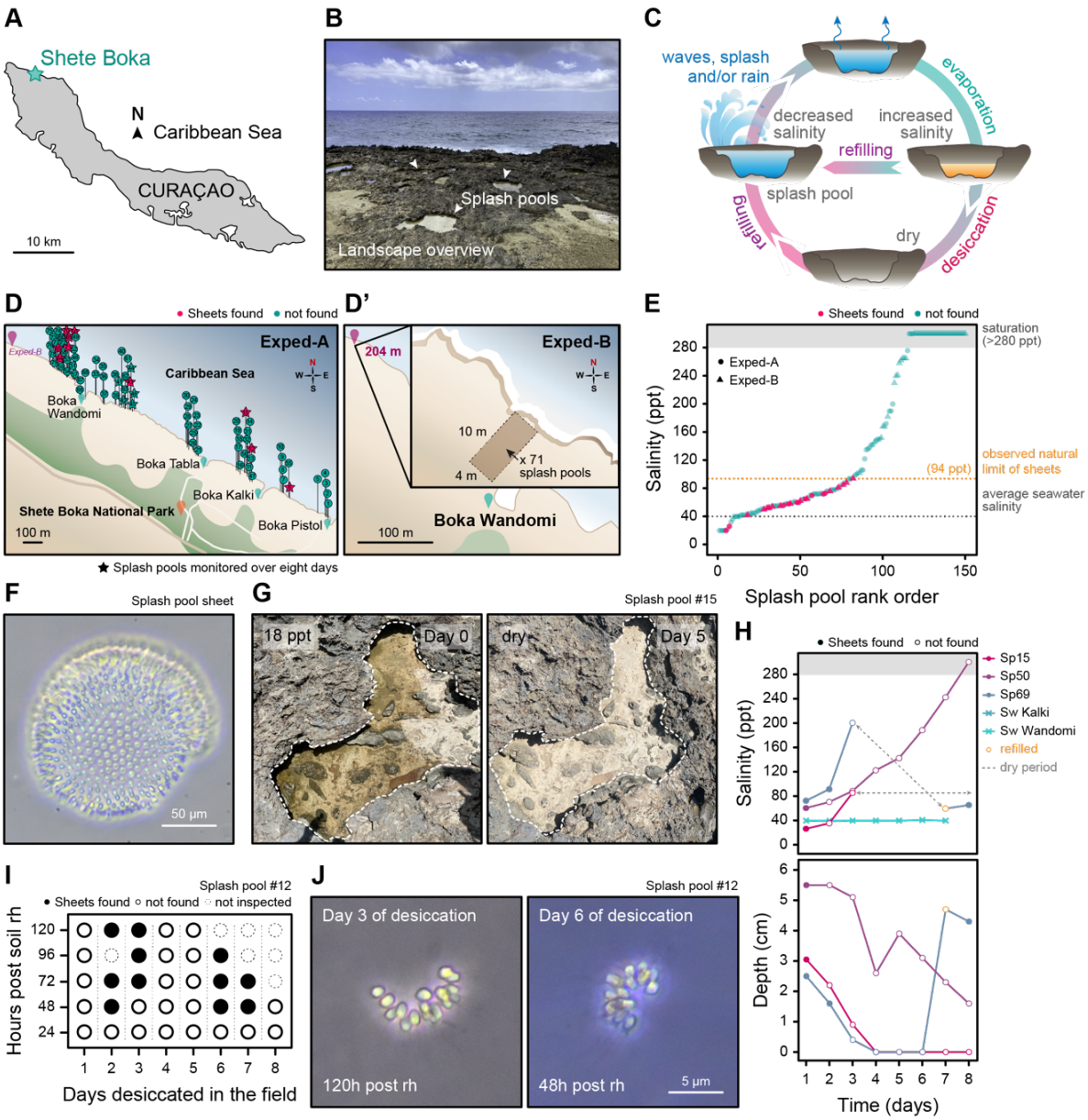

Figure 3. Cyclical salinity fluctuations constrain the occurrence of multicellular *C. flexa* sheets in their natural environment. (A) Map of Curaçao and location of Shete Boka National Park (turquoise star) where fieldwork data was collected in Exped-A and Exped-B expeditions (12° 22' 5.718" N, 69° 06' 56.916" W). (B) Representative photograph of the landscape in Shete Boka, including splash pools where *C. flexa* sheets can be found (white arrowheads). (C) Schematics of a splash pool natural cycle of seawater evaporation, desiccation, and refilling. (D) Maps showing the locations of sampled splash pools in Exped-A and in Exped-B expeditions. In Exped-A (D), samples were collected from splash pools along ~2 km of Shete Boka coastline (n=79). 15 of these splash pools were randomly selected for daily monitoring during eight days (stars) (shown are results from the first day of monitoring). Colors indicate whether sheets were found (magenta) or not found (turquoise) upon microscopic inspection. In Exped-B (D'), a random number generator was used to select the randomized sampling location (purple pin, 204 m upstream of Boka Wandomi). Samples were collected from splash pools within an area of 10 m by 4 m (n=71). (E) Distribution of salinity of splash pools surveyed in Exped-A (circles) and Exped-B (triangles). For daily monitored splash pools, measurements from the first day of monitoring are shown. Magenta and turquoise colors indicate that sheets were

respectively found and not found in splash pool samples. The observed natural limit of salinity where sheets were found (94 ppt) is indicated by an orange dotted line, and the average seawater salinity measured in the *bokas* with a gray dotted line. Gray area: salinity saturation (>280 ppt). (F) Brightfield image of a sheet observed in a splash pool sample. (G) Representative images of a splash pool near Boka Kalki (Sp15) followed for eight days, showing recorded salinity in the upper left. This splash pool was completely desiccated at day 5 (right). Dashed line: splash pool outline. (H) Salinity (upper panel) and depth (lower panel) measurements in three representative splash pools followed over eigth days. Shown are one splash pool that experienced evaporation but not complete desiccation (Sp50), one splash pool that experienced complete desiccation (Sp15), and one splash pool that experienced both desiccation and refilling (Sp69). Filled and empty circles indicate that sheets were respectively found and not found in splash pool samples. Gray area: salinity saturation. Dashed lines: dry periods. Orange circles: refilling events. (I) Recovery of sheets from soil samples collected from a splash pool (Sp12) during its dry period. Soil samples were collected every day for eight days and were independently rehydrated in the laboratory with filtered seawater from the *bokas,* reconstituting salinity back to 42 ppt. Each rehydrated soil sample was monitored over five days for sheet re-appearance. Filled circle: sheets observed. Empty circle: sheets not observed. Dashed empty circle: sample not inspected. rh: rehydration. (J) Brightfield images of soil-recovered sheets (same experiment as in I) collected after 3 (left) and 6 (right) days of desiccation and rehydrated in the laboratory (lower left: time post-rehydration). Figure related to **Figures S4-S7**, **movies S14-S16**, **Tables S1-S2** and **Supplementary Files S1-S4**.

Transitions into and out of multicellularity correlate with the natural evaporation-refilling cycle of splash pools

We then set out to study the natural evaporation-refilling cycle of splash pools and how it may impact the presence/absence of sheets. We monitored ten splash pools in which *C. flexa* sheets were found and five more randomly selected splash pools daily over eight days (**Figures 3G-H and S6**). We screened samples for sheets once per day and measured the salinity and maximum depth of each splash pool (**Figures 3G-H and S6**). We observed a gradual decrease in depth and concomitant increase in salinity in all 15 splash pools (presumably due to evaporation; **Figure S6A-B**), six events of complete desiccation (**Figure S6C-D**), and four events of refilling (**Figure S6E-F**; see three examples in **Figure 3H**). In all cases, *C. flexa* sheets were no longer observed after salinity crossed a ~100 ppt threshold during gradual evaporation (**Figures 3H and S6**), consistent with results from Exped-A and Exped-B (**Figures 3E-H and S6**). Moreover, artificial evaporation of a natural splash pool sample containing sheets in the laboratory led to sheet disappearance (**Figure S7**). These observations further reinforced the idea that the multicellular form of *C. flexa* might not tolerate high salinity levels.

Interestingly, in two dry splash pools that underwent refilling during our study (restoring salinity down to ~50 ppt), sheets were re-observed 48 hours after refilling (Sp69 and Sp70; **Figures 3H and S6E-F**). The new incoming sheets may have arrived from waves or splash,

318 or may have been transferred from neighboring splash pools. Alternatively, *C. flexa* might
319 have persisted in the soil of desiccated splash pools in a hitherto unrecognized resistant form,
320 perhaps in the form of unicellular cysts (which have been morphologically reported in other
321 choanoflagellates (*50*–*55*)). Under this hypothesis, colonies would disassemble and transition
322 into resistant single cells under high salinity, and those cells would then develop back into
323 sheets once salinity decreased. To explore this possibility *in situ*, we collected soil samples
324 from six desiccated splash pools in which *C. flexa* had been previously observed, rehydrated
325 them in the lab (down to ~65 ppt salinity) and monitored the rehydrated samples for several
326 days (**Figure 3I-J; movie S16**). Surprisingly, sheets could be recovered in various soil
327 samples collected from one splash pool after two to seven days of desiccation (**Figure 3I-J**).
328 Sheets consistently appeared 48-72 hours post-rehydration, suggesting that a resistant form
329 of *C. flexa* can survive complete desiccation in the wild for at least a week (**Figure 3I-J**).
330 Interestingly, the presence of choanoflagellates in soil might be a more general phenomenon:
331 metagenomic analyses of soil samples from diverse environments have revealed the
332 presence of choanoflagellate species yet to be studied (*56*, *57*), which might represent a
333 significant and poorly understood ecological niche for choanoflagellates (*58*).
334 Given that salinity fluctuations in splash pools seemed to dramatically impact *C. flexa*
335 multicellularity in nature, we next set out to investigate the phenotypic response of *C. flexa* to
336 evaporation-refilling cycles in a laboratory context.
337

338 **Experimental evaporation-refilling cycles cause reversible transitions into and**
339 **out of multicellularity**

340

341 To better understand the response of *C. flexa* to evaporation, desiccation, and refilling, we
342 designed an experimental setup mimicking the natural evaporation-refilling cycles of Shete
343 Boka splash pools (**Figures 4A and S8**). As a first step, we calculated the empirical
344 evaporation rate of 12 splash pools in our longitudinal field survey (see methods; **Figure S8A-**
345 **B**). We then subjected *C. flexa* cultures to evaporation in an incubator (**Figure S8C**), matching
346 both the temperature (30°C) and evaporation rate to that observed in natural splash pools
347 (see methods; **Figure S8D**). This setup resulted in complete desiccation after four days of
348 evaporation (starting from artificial seawater (ASW) with a salinity of 35 ppt, referred to as 1X
349 salinity in the rest of the text). Under these conditions, *C. flexa* sheets gradually dissociated
350 into non-motile single cells (**Figures 4A-B and S9; movie S17**), with more than 50% of the
351 cells being solitary when salinity crossed the limit of sheet occurrence observed in the field

352 (94 ppt; **Figures 3E and 4A**). Almost all sheets had dissociated into single cells when salinity
353 reached saturation (**Figures 4A-B and S9; movie S17**). As a negative control, we monitored
354 identically treated cultures that were not undergoing evaporation and observed that colonies
355 remained multicellular throughout the experiment (**Figure S10**). This suggested that sheet
356 dissociation in the gradual evaporation setup was caused by the increasing salinity. To
357 independently test this hypothesis, we raised the salinity of *C. flexa* cultures by directly adding
358 seawater salt (without evaporation) and similarly observed dissociation of multicellular sheets
359 into single cells (**Figure S11A-C**).
360 To test whether single cells resulting from sheet dissociation in the lab were viable and
361 could survive desiccation, we mimicked splash pool refilling by rehydrating gradually
362 evaporated samples with artificial seawater three hours after full desiccation. This brought
363 salinity back down to ~50 ppt and was followed by the reappearance of small sheets as soon
364 as 24 hours post-rehydration. The fraction of cells in colonies increased gradually until ~50%
365 of cells were colonial on day 7 and ~75% on day 9 (**Figure 4A-B**).
366

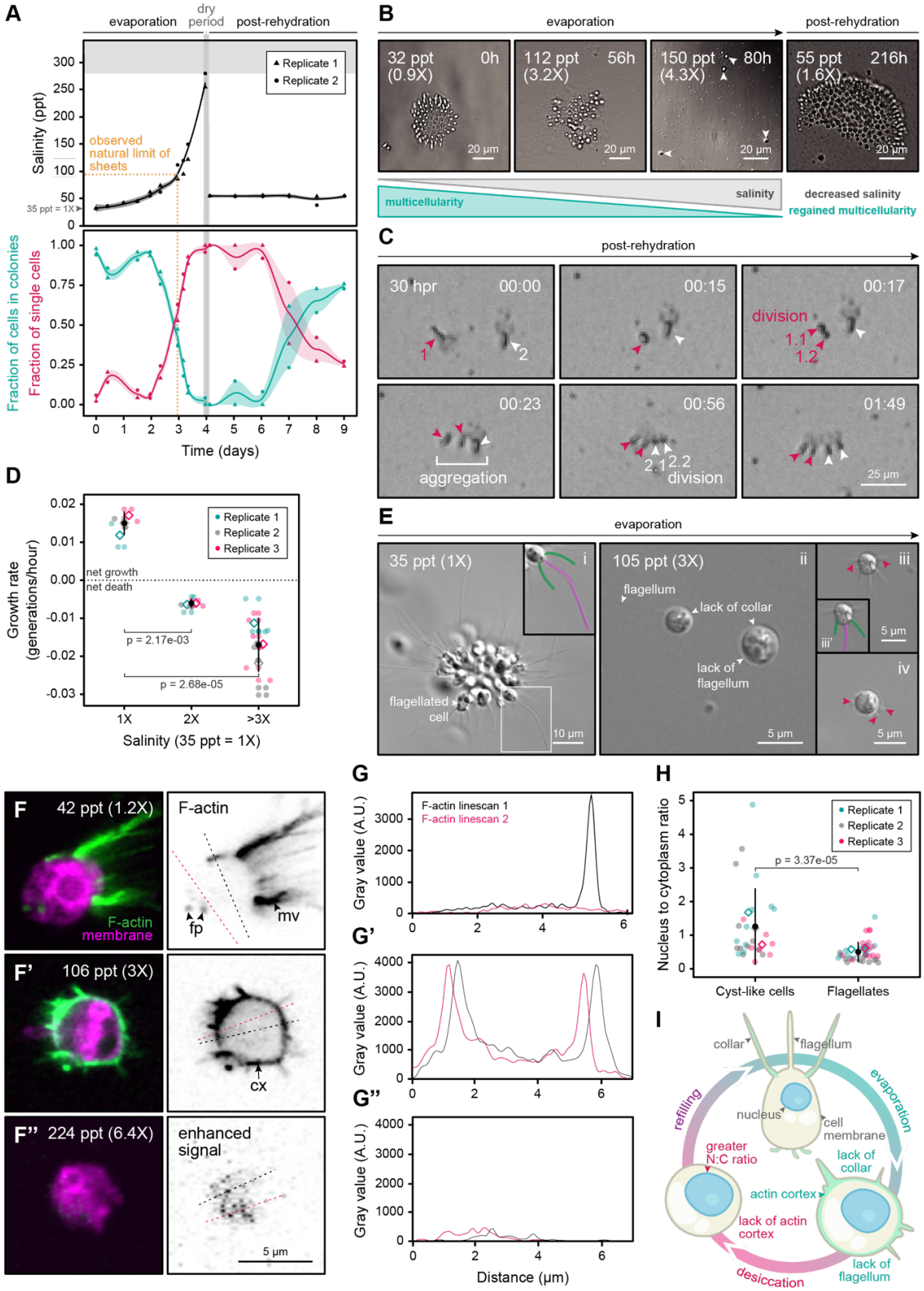

(Figure 4 legend on the next page)

369 **Figure 4. Experimental evaporation-refilling cycles causes reversible transitions between multicellular sheets and**
370 **unicellular cyst-like cells.** (A) Quantification of salinity (upper panel) and fraction of cells in colonies (magenta) or in single cells
371 (turquoise) (lower panel) during a 9-day gradual evaporation time course. Dark gray rectangle: complete desiccation (dry period).
372 Orange dotted line: observed natural salinity limit of sheet occurrence. Gray area: salinity saturation. Lines correspond to mean
373 values and shadowed area to standard deviation. Experiment performed in two independent biological replicates. (B) Stills of *C.*
374 *flexa* sheets during the same 9-day gradual evaporation timecourse in A, showing salinity (in ppt and fold-change compared to
375 that of 1X ASW in parenthesis, upper left) and time (upper right). Sheets had completely dissociated into single cells (white
376 arrowheads) after 80 hours of gradual evaporation. Multicellular sheets were observed again after complete desiccation and
377 rehydration with 1X ASW. (C) Stills from a brightfield timelapse movie of cells rehydrated after complete desiccation. Recovered
378 flagellate cells re-form colonies both by clonal division and aggregation 30 hours after rehydration. (D) Growth rate of cells at
379 different salinities during gradual evaporation in three independent biological replicates. Black circles: mean. Error bars: standard
380 deviation. n=28, *p* by the Mann-Whitney U test. Diamonds: mean values of independent biological replicates. (E) Brightfield
381 images of *C. flexa* showing morphological changes during gradual evaporation. At ~1X seawater salinity (left), *C. flexa* occurs in
382 the form of multicellular sheets of flagellated cells (i). Green pseudocolor: collar. Magenta pseudocolor: flagellum. During gradual
383 evaporation (ii-iv, right panel), sheets dissociate into unicellular cyst-like cells. Cyst-like cells lack a collar, often lack a flagellum,
384 and can exhibit filopodia-like protrusions (magenta arrowheads in iii-iv). (F) AiryScan micrographs of *C. flexa* cells fixed during
385 gradual evaporation and stained with a membrane (FM^{TM} 4-64FX, magenta) and F-actin (phalloidin Alexa 488, green) dyes,
386 showing lack of collar and flagellum in cyst-like cells. A flagellate cell (F, low-evaporation control) exhibits distribution of F-actin
387 distribution in the collar of microvilli (mv, black arrowhead) and filopodia (fp, black arrowhead). Gradual evaporation triggers a
388 morphological change from a flagellate to a cyst-like cell, showing a transient actin cortex (cx) at early stages of evaporation (F',
389 black arrow) which disappears as salinity approaches saturation (F''). (G) (resp. G', G") Line scan of F-actin fluorescence intensity
390 along the dashed lines of interest in F (resp F', F"), showing cortical actin as two peaks where the lines intersect the cell cortex.
391 (H) Quantification of the nucleus-to-cytoplasm ratio in cyst-like cells (n=27) and flagellate cells (n=38) in three independent
392 biological replicates. Black circles: means. Error bars: standard deviations. Diamonds: mean values of independent biological
393 replicates. *p* by the Mann-Whitney U test. (I) Schematic summarizing phenotypic changes experienced by *C. flexa* cells during
394 gradual evaporation. At early stages of evaporation (turquoise), flagellate cells differentiate into cyst-like cells by losing their
395 collar and flagellum, and show a temporal actin cortex. At later stages of evaporation (desiccation, magenta), cyst-like cells lack
396 an actin cortex and show a higher nucleus-to-cytoplasm ratio. Rehydration (refilling, purple) induces a cyst-like cell-to-flagellate
397 cell transition, where cells regenerate their collar and flagellum and re-form multicellular sheets. Figure related to **Figures S8-**
398 **S14** and **movies S17-S18**.
399
400 We assessed the mechanism of colony re-formation by time-lapse microscopy of
401 desiccated cultures after rehydration and captured instances of unicellular flagellates
402 engaging in both clonal and aggregative multicellular development (**Figure 4C; movie S18**).
403 Taken together, our results show that *C. flexa* sheets dissociate into non-motile single cells
404 during gradual evaporation, that these solitary cells can survive complete desiccation under
405 laboratory conditions, and that sheets reform after rehydration through both clonal division
406 and aggregation. These findings are consistent with our field observations, where we
407 recovered sheets after rehydrating soil samples from a dry splash pool (**Figure 3I-J**), and
408 further support the existence of a desiccation-resistant form of *C. flexa*.
409
410

411 ***C. flexa* differentiates into solitary cyst-like cells at high salinity**

412

413 We then set out to further investigate the phenotype of the desiccation-induced single
414 cells. In diverse protists, resistance to desiccation is often achieved by differentiation into cysts
415 (*59–61*), which are dormant cells with reduced metabolic activity and minimal or arrested
416 proliferation. This process, known as encystment, often entails significant morphological
417 changes such as rounding of the cell body, changes in cell volume, flagellar loss, and
418 formation of a protective cell wall (*53*, *59*, *62–68*). First, we determined whether *C. flexa*
419 desiccation-resistant cells (hereafter 'cyst-like cells') actively proliferate by quantifying cell
420 growth during gradual evaporation in the laboratory. We found that growth was arrested above
421 2X salinity, with net cell loss above 3X salinity (**Figures 4D and S12**). These effects may be
422 attributable to a halt in the cell cycle and cell death due to hypersaline stress, similar to
423 processes observed during encystment in other protists (*13*, *59*, *62*, *68*, *69*).

424 We next monitored cellular morphology by DIC microscopy during gradual evaporation
425 and observed structural changes that occurred asynchronously, resulting in a heterogeneous
426 cell population (**Figure 4E**). At 3X salinity, most cells had dissociated from their colonies and
427 bore a round cell body lacking microvilli and, most often, lacking a flagellum (**Figure 4Eii**).
428 Additionally, some cells exhibited multiple filopodia-like protrusions (**Figure 4Eiii**). Membrane
429 and F-actin staining of cyst-like cells confirmed that they lacked a collar complex (**Figures 4F**
430 **and S13**) but also revealed that they transiently formed an F-actin cortex, detectable at 3X
431 salinity but lost above 6X (close to saturation; **Figures 4F-G and S13**). This transient actin
432 cortex might contribute to protecting the plasma membrane against osmotic stress during the
433 initial differentiation stages (*70–73*).

434 Finally, morphometric analysis of cell body and nucleus volume showed that cyst-like cells
435 had a larger nucleus-to-cytoplasm ratio compared to flagellate cells cultured in 1X salinity
436 (p=3.4e-05; **Figures 4H and S14**). An increase in the nucleus-to-cytoplasm ratio frequently
437 correlates with cell quiescence in other systems (*74*), consistent with the growth arrest in *C.*
438 *flexa* cyst-like cells (**Figures 4D and S12**). To confirm that these changes were induced by
439 hypersaline stress, we directly increased the salinity of *C. flexa* cultures by addition of
440 seawater salt, and observed similar morphological changes and arrest in cell growth (**Figure**
441 **S11**).

442 In sum, hypersalinity caused drastic and reversible changes in cell architecture and
443 growth: loss of the collar and flagella (and thus of motility), formation of a transient actin cortex,
444 increased nucleus-to-cytoplasm ratio, and arrest of cell growth (**Figure 4I**), resembling the

445 changes that occur during encystment in diverse protists (*59*, *62*). Thus, during the
446 evaporation-refilling cycle of a splash pool, *C. flexa* likely alternates between a multicellular
447 flagellated form (at low salinity) and a unicellular cyst-like form (at high salinity), suggesting
448 these two phenotypes benefit from an adaptive advantage in their respective environment.
449 We thus decided to directly test for these putative advantages in laboratory conditions.
450

451 **Multicellular sheets are advantaged at low salinity and unicellular cyst-like**
452 **cells are advantaged at high salinity**

453

454 If *C. flexa* cyst-like cells represent a desiccation-resistant form, we could expect these
455 cells to be more resistant to hypersaline stress and desiccation compared to sheets. To test
456 this, we compared the survival of both sheets and cyst-like cells after desiccation. We
457 subjected sheets to fast evaporation, which resulted in complete desiccation from 1X salinity
458 over 20 hours (see methods). Under these conditions, cells did not acquire a cyst-like
459 morphology but instead retained an observable flagellum, collar, and multicellular morphology
460 even after complete desiccation (**Figure S15**). This suggests that the formation of cyst-like
461 cells requires gradual evaporation at a comparable rate to that of natural splash pools. In
462 parallel, we induced the differentiation of *C. flexa* into cyst-like cells by slow evaporation
463 following the protocol detailed in the previous section (from 1X salinity to desiccation in 72
464 hours). After desiccation, we rehydrated both types of cells by adding 1X ASW and monitored
465 their recovery. We found that desiccated sheets having undergone rapid evaporation never
466 developed into viable cells after rehydration (**Figure 5A**). By contrast, as in the experiments
467 detailed earlier, rehydrated cyst-like cells consistently gave rise to viable sheets, confirming
468 that they had survived desiccation (**Figure 5A**). These observations show that cyst-like cells,
469 unlike flagellates, are equipped to survive hypersalinity and desiccation, and suggest that
470 differentiation into cyst-like cells confers a selective advantage during evaporation. The loss
471 of multicellularity during differentiation into cyst-like cells is likely linked to the retraction of the
472 microvillous collar that connects cells within sheet colonies.
473

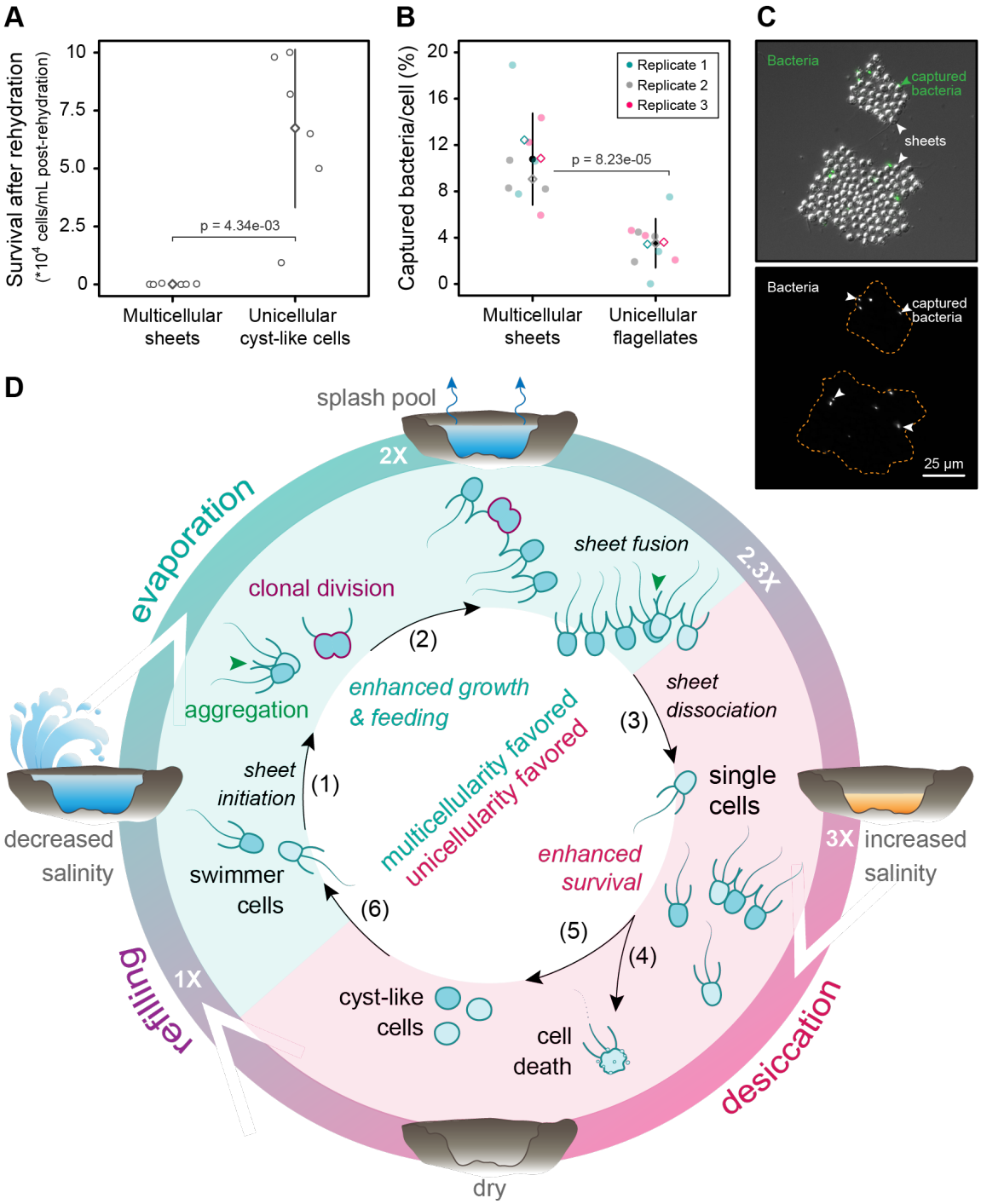

Figure 5. Unicellular cyst-like cells are advantaged at high salinity while multicellular sheets are advantaged at low salinity. (A) Quantification of cell survival after 12 hours of desiccation in multicellular sheets (n=6 technical replicates) to unicellular cyst-like cells (n=6 technical replicates). Diamonds: means. Error bars: standard deviations. *p* by the Mann-Whitney U test. (B) *C. flexa* multicellular sheets are more efficient at capturing bacteria than unicellular flagellates. Number of labelled bacteria captured per flagellate cells in multicellular colonies (n=9) or in cultures of unicellular flagellates (n=9) in three independent biological replicates. Black circles: means. Error bars: standard deviations. Diamonds: means of independent biological replicates. *p* by the Mann-Whitney U test. (C) DIC images of multicellular sheets (upper panel, white arrowheads)

483 capturing fluorescently-labelled bacteria using Bactoview dye (upper panel: green; lower panel: white). (D) Summary schematic
484 of *C. flexa* mixed clonal-aggregative development entrained by natural splash pool evaporation-refilling cycles. Multicellularity is
485 favored in low salinity, where sheets exhibit enhanced growth and prey capture (turquoise): (1) unicellular flagellate cells can
486 aggregate and/or divide clonally to initiate multicellular sheet development; (2) sheets expand by clonal cell division, by
487 aggregation of individual cells, and by sheet fusion. Gradual evaporation leads to increase in salinity and favors unicellularity
488 (magenta): (3) *C. flexa* remains multicellular in up to 2.3-fold salinity, but hypersaline conditions (>3-fold salinity) trigger sheet
489 dissociation into single cells that are incapable of proliferation and occasionally to cell death (4). Gradual evaporation, instead,
490 results in the differentiation of flagellates into cyst-like cells (5) capable of surviving desiccation. (6) Rehydration restores
491 permissive salinity and induces differentiation of cyst-like cells into flagellates, which undergo clonal-aggregative multicellular
492 development. Figure related to **Figure S15**.
493

494 Because unicellular cyst-like cells seemed to have a survival advantage over multicellular
495 flagellates in the hypersaline phase of the evaporation-refilling cycle, we wondered whether
496 multicellularity, by contrast, was advantageous in the other phase of the cycle, marked by low
497 salinity. It has been speculated that multicellularity in choanoflagellates might enhance
498 feeding via cooperative hydrodynamic interactions between flagella, increasing the flux of
499 bacterial prey towards the collar (*75*–*77*); however, this concept remains uncertain in the
500 model choanoflagellate *Salpingoeca rosetta*, with different studies having come to contrasting
501 conclusions (*75*, *78*, *79*). To test for a feeding advantage in multicellular sheets of *C. flexa*,
502 we quantified the capture of fluorescent bacteria in sheets and dissociated single flagellates
503 (**Figure 5B-C**). We found that sheets captured more than twice as many fluorescent bacteria
504 per cell as single cells (**Figure 5B-C**). This suggests that multicellularity confers a prey capture
505 advantage at the salinity levels that are compatible with cells maintaining a functional collar
506 complex and, therefore, with feeding.
507 Taken together, our findings support a model of *C. flexa* life history that correlates with the
508 evaporation-refilling cycle of splash pools characteristic of their natural habitat (**Figure 5D**).
509 *C. flexa* sheets are found in water-filled splash pools with salinities below ~2.3-fold that of
510 natural seawater. As gradual evaporation proceeds, salinity increases, and sheets dissociate
511 and differentiate into solitary, non-motile, and non-proliferative cyst-like cells (some of which
512 undergo cell death). These cyst-like cells can survive complete desiccation and persist in the
513 soil of the splash pools. After splash pool refilling, cyst-like cells regrow a collar complex and
514 transition back into free-swimming flagellates that develop into multicellular sheets by
515 aggregation and/or clonal division, a phenotype that more efficiently captures bacteria and
516 presumably supports faster cell proliferation.
517

Discussion

The ecological context of *C. flexa* clonal-aggregative multicellularity

Our results show that *C. flexa* can form multicellular sheets through a combination of clonal division and aggregation following the rehydration of desiccated cyst-like cells. This mixed developmental strategy might represent an adaptation to the ephemeral nature of water-filled splash pools, allowing faster multicellular development by simultaneous action of both mechanisms. It might also serve as a versatile strategy for robust re-establishment of multicellularity across a broad range of environmental conditions: indeed, aggregative and clonal multicellularity are subjected to different constraints, as they respectively depend on cell density and on the possibility of cell division (which is in turn constrained by salinity and availability of bacterial prey). In our laboratory experiments, *C. flexa* appeared capable of both purely clonal development (at low cell density and under permissive conditions for proliferation) and purely aggregative development (at sufficient cell density, even if proliferation is compromised), as well as intermediate modes.

The selective advantage of multicellularity has been the subject of intense debates (*76*, *80–82*) and multiple studies in choanoflagellates (*75*, *76*, *83–87*). In the case of *C. flexa*, the prey capture efficiency of cells within sheets surpasses that of solitary flagellated cells, suggesting a feeding (and likely reproductive) benefit of multicellularity. Cooperative feeding—a trait observed among various protists—has been postulated as a selective factor for the evolution of multicellularity (*88*). However, other advantages of multicellularity might exist in *C. flexa*. Prominently, *C. flexa* colonies exhibit collective behavior through coordinated contractility that implements whole-colony inversion. Inversion allows reversible transitions between feeding and swimming states and is modulated by several signals, including mechanical stimuli, heat shocks, and nitric oxide (*37*). This switch is also regulated by light-to-dark transitions, thus enabling photokinesis (preferential accumulation of sheets under light) (*35*). Our previous research indicates that individual cells from dissociated sheets are no longer capable of photokinesis, suggesting this behavior requires multicellularity (*35*). Moreover, multicellular groups show decreased vulnerability to size-selective predators in different protists and predator avoidance has been proposed as a potential selective force for evolving multicellularity (*6*, *15*, *76*, *81*) (but see (*86*)).

More generally, the environmentally entrained life history transitions of *C. flexa* are in line with other recently described examples. Unicellular-to-multicellular switches are controlled by fluctuating environmental parameters in other species, such as salinity for cyanobacteria in brackish environments (*89*) and periodic flooding for cave bacteria attached to surfaces (*90*). A selective advantage for regulated life cycles in fluctuating environments has also been supported by laboratory experiments in yeast (*91*) and by theoretical models (*5*, *92*, *93*). The phenotypic plasticity of *C. flexa* might thus enable it to reap both the benefits of multicellularity (for feeding and collective behavior) under permissive conditions, and of differentiation into solitary cyst-like cells for individual survival under harsh conditions.

Evolutionary implications of mixed clonal-aggregative multicellularity

The clonal-aggregative multicellularity of *C. flexa* contrasts with that of previously characterized multicellular choanoflagellates, which appear to develop solely clonally (*3*, *23*, *24*, *26*, *94–98*). Indeed, the best-characterized example is the formation of rosette colonies in *S. rosetta*, which occurs by serial cell division without separation of sister cells and thus requires cell proliferation (*24*). *S. rosetta* can also develop into chain colonies, which are similarly thought to form clonally (*25*, *26*).

Beyond choanoflagellates, both clonal and aggregative multicellularity are widely present, with a discontinuous occurrence, across unicellular holozoans (*99–104*, *28*, *42*, *27*, *29*, *30*) and eukaryotes as a whole (*3*, *105–107*). The scattered distribution of clonal and aggregative multicellularity is currently interpreted as reflecting independent evolutionary origins of both types of development (*4*).. However, the discovery of clonal-aggregative multicellularity in a eukaryote raises the intriguing alternative possibility of evolutionary interconversions between aggregative and clonal multicellular development (via a mixed intermediate). Future studies of clades that contain both clonal and aggregative forms (such as Holozoa and Holomycota) might help test this possibility. Although mixed clonal-aggregative multicellularity has not been formally reported before in other protists to our knowledge, some parallels can be drawn with processes described in other taxa or contexts: for example, clonality and aggregation might cooperate in the formation of bacterial boofilms (*108*) and in the development of (unicellular but multinucleated) syncytia in reticulopodial amobae (*1*). This raises the possibility that mixed clonal-aggregative development might be more widespread than currently appreciated.

583 Interestingly, the phenotype of *C. flexa* colonies differs in some important respects
584 from that of most previously described aggregative structures. The paradigmatic model of
585 aggregative multicellularity is fruiting body formation (see glossary), which has been well-
586 characterized in dictyostelid amoebae (*4*, *14*, *109*) and evolved convergently multiple times
587 across eukaryotes (*110*, *111*) (and even at least once in bacteria (*112*)). Fruiting bodies are
588 masses of dormant cells (sometimes together with cells having undergone cell death) that
589 disperse into single cells before resuming metabolic activity and proliferation upon the
590 restoration of favorable environmental conditions. By contrast, *C. flexa* sheets are
591 proliferatively and behaviorally active, and appear to survive and reproduce in a multicellular
592 form as long as permissive conditions persist. Thus, the ecological niche accessible to mixed
593 clonal-aggregative multicellularity might differ from that typical of purely aggregative forms.
594
595 Aggregative multicellularity comes with a well-known evolutionary challenge: one
596 aggregate can combine cells of different ancestries and potentially different genotypes, thus
597 raising the possibility of conflict (*113*–*115*). Aggregates are notably vulnerable to cheater
598 genotypes, which reap the benefits of multicellularity without contributing their fair share of the
599 cost of multicellular development. Such cheaters have, for example, been described in
600 *Dictyostelium* (*116*), in the fruiting body-forming bacterium *Myxococcus* (*117*), and in
601 flocculating yeast (*10*). The evolutionary challenge posed by cheater mutants can be
602 addressed by strategies that limit aggregation to fellow co-operators, either directly by co-
603 operator recognition (so-called "green beard" mechanisms (*118*, *119*)) or indirectly by
604 preferential aggregation with close relatives. Restriction of aggregation to relatives can either
605 be enforced actively by kin recognition (mediated by polymorphic loci (*120*–*122*)) or be
606 facilitated passively by spatial structuration of the environment that can limit dispersal (*123*,
607 *124*). The latter might be relevant to *C. flexa*, as splash pools are collections of disconnected
608 environments that might lead to geographic divergence of genotypes (as shown for other
609 organisms in similar environments, such as *Daphnia* metapopulations in tide pools (*125*)).
610 Splash pools might thus favor the evolution of aggregative multicellularity by mitigating the
611 need for strong kin recognition mechanisms. This is in line with recent models supporting an
612 “ecological scaffolding” function for patchy environments in the emergence of multicellularity
613 (*126*). In the future, studies of potential kin recognition mechanisms, natural genetic diversity
614 and dispersal in *C. flexa* might shed further light on these questions.
615
616

Conclusion

Our study documents an unusual mode of multicellular development that combines features of clonal and aggregative multicellularity in a choanoflagellate, belonging to the sister-lineage of animals. This complex life cycle further underscores the emerging concept of considerable phenotypic and developmental plasticity among close unicellular relatives of animals, supporting the existence of a complex life cycle in unicellular ancestors of animals (*19*, *127*).

Beyond this, our study establishes *C. flexa* as a model to study the facultative multicellular development of a close relative of animals in its natural context. This contrasts with other well-characterized facultatively multicellular holozoans, such as *S. rosetta* (*20*) and *C. owczarzaki* (*128*), which could both be isolated only once from their natural environment and in which studies of unicellular-to-multicellular transitions are thus inevitably restricted to laboratory setups. In the future, we expect the dialogue between field and lab studies of *C. flexa* to continue, clarifying questions such as the selective advantage(s) and ecological implications of multicellularity and unicellularity, as well as the existence of possible natural kin recognition mechanisms and cheater mutants.

Acknowledgements

We thank the personnel of the Shete Boka National Park in Curaçao for access to the field site. We thank Tess Linden for help during preliminary field work experiments and feedback on the manuscript. We thank Marvin Albert, Stéphane Rigaud and Jean-Yves Tinevez at the Image Analysis Hub at the Institut Pasteur for feedback on image analyses. We acknowledge Pierre-Henri Commere and Sebastien Megharba from the Flow Cytometry platform at Institut Pasteur for support with single-cell isolation of new *C. flexa* isolates by flow cytometry. Special thanks to Geneviève Milon and Noah Whiteman for feedback and useful discussions on laboratory and fieldwork experimental design, respectively. We also thank members of Brunet and King laboratories for feedback and useful discussions and Jaime Ramirez and Kayla Dinshaw for technical support during preliminary experiments. NRR is supported by the European Union's Horizon Europe research and innovation funding program under a Marie Skłodowska-Curie Actions grant (Grant Agreement ID: 101106415). JRR is supported by a National Science Foundation Graduate Research Fellowship Program (grant no. 1752814). NK and work in the King lab is supported by the Howard Hughes Medical Institute. TB and work in the Brunet lab is supported by the Institut Pasteur (G5 package), the CNRS (UMR

3691), and by the ERC Starting Grant EvoMorphoCell (Grant agreement ID: 101040745). Funded by the European Union. Views and opinions expressed are however those of the author(s) only and do not necessarily reflect those of the European Union or the European Research Council. Neither the European Union nor the granting authority can be held responsible for them.

Author contributions

Conceptualization: NRR, JRR, TB. Methodology: NRR, JRR, BTL, MCC, EATH, TB. Validation: NRR, JRR, BTL, MCC, TB. Investigation: NRR, JRR, YF, CC, TB. Data analysis: NRR, JRR, YF, TB. Writing – original drafting: JRR with help from NRR and TB. Writing – editing: BTL, MCC, MJAV. Figure preparation: NRR with help from JRR and TB. Supervision: NK, TB. Project administration: NK, TB. Funding acquisition: NRR, JRR, NK, TB.

Competing interests

The authors declare no competing interests.

Materials and Methods

See detailed Materials and Methods in the **Supplementary Information** file.

Supplementary Material

Supplementary Figures S1-S15, Table S2 and legends for Table S1, Supplementary Files S1-S4 and Supplementary Movies S1-S18 are provided in the **Supplementary Information** file.

674 **Box 1. Glossary**

675

676 **Cheaters**: in social evolution theory, organisms that receive a benefit at the cost of other
677 organisms of the same species within the context of a collective behavior. In the case of
678 aggregative multicellularity, cheaters are cells within a chimeric multicellular aggregate that
679 impair collective outcomes to their own benefit. For example, in sorocarp-forming eukaryotes,
680 cheaters differentiate disproportionately into spores (reproductive cells) rather than other cell
681 types (such as stalk cells), giving them a higher likelihood of reproducing than non-cheaters.
682 Cheaters can exploit shared resources in a way that enhances their own fitness at the
683 expense of the collective. The existence of cheaters may impede group-level selection of traits
684 and result in evolutionary conflict (*116*, *117*).

685

686 **Fruiting body:** a spherical mass of stress-resistant cells (spores or cysts), often in a quiescent
687 state, that eventually undergoes disassembly and dispersal (*129*). Fruiting bodies often result
688 from aggregative development and are sometimes equipped with a stalk providing elevation
689 from the substrate, and facilitating dispersal by the wind after dissociation.

690

691 **Holozoa:** eukaryotic clade encompassing all species more closely related to animals than to
692 fungi. Holozoa comprises various clades, including Metazoa (animals), Choanoflagellata,
693 Filasterea, Corallochytrea/Pluriformea, and Ichthyosporea. Unicellular eukaryotes (*a.k.a.*
694 protists) within the Holozoa clade are pivotal for elucidating the evolutionary transitions that
695 facilitated the emergence of multicellularity in animals from unicellular ancestors (*27*, *130*, *38*).

696

697 **Splash pools:** shallow seawater pools in rocky shores inhabited by prokaryotic and
698 eukaryotic organisms that are occasionally filled with seawater by oceanic waves and splash
699 (and sometimes with rainwater). In Curaçao, the substrate of splash pools is composed mainly
700 of limestone. Their sizes range from a few centimeters to a few meters. In splash pools,
701 environmental conditions such as seawater volume, temperature, salinity, and oxygen
702 fluctuate as they undergo natural evaporation-refilling cycles over a few days or weeks. Thus,
703 splash pools are considered extreme environments.

704

705

References

1. Ł. Lamża, Diversity of 'simple' multicellular eukaryotes: 45 independent cases and six types of multicellularity. *Biological Reviews* **98**, 2188–2209 (2023).
2. R. K. Grosberg, R. R. Strathmann, The Evolution of Multicellularity: A Minor Major Transition? *Annual Review of Ecology, Evolution, and Systematics* **38**, 621–654 (2007).
3. T. Brunet, N. King, The Origin of Animal Multicellularity and Cell Differentiation. *Developmental Cell* **43**, 124–140 (2017).
4. J. T. Bonner, The origins of multicellularity. *Integrative Biology* **1**, 27–36 (1998).
5. M. Staps, J. Van Gestel, C. E. Tarnita, Emergence of diverse life cycles and life histories at the origin of multicellularity. *Nat Ecol Evol* **3**, 1197–1205 (2019).
6. M. L. F. Velicer Kaitlin A. Schaal, Gregory J., "Group Formation: On the Evolution of Aggregative Multicellularity" in *The Evolution of Multicellularity* (CRC Press, 2022).
7. P. Márquez-Zacarías, P. L. Conlin, K. Tong, J. T. Pentz, W. C. Ratcliff, Why have aggregative multicellular organisms stayed simple? *Curr Genet* **67**, 871–876 (2021).
8. A. H. Knoll, The Multiple Origins of Complex Multicellularity. *Annual Review of Earth and Planetary Sciences* **39**, 217–239 (2011).
9. R. M. Fisher, C. K. Cornwallis, S. A. West, Group Formation, Relatedness, and the Evolution of Multicellularity. *Current Biology* **23**, 1120–1125 (2013).
10. J. T. Pentz, P. Márquez-Zacarías, G. O. Bozdag, A. Burnetti, P. J. Yunker, E. Libby, W. C. Ratcliff, Ecological Advantages and Evolutionary Limitations of Aggregative Multicellular Development. *Current Biology* **30**, 4155-4164.e6 (2020).
11. J. M. Biernaskie, S. A. West, Cooperation, clumping and the evolution of multicellularity. *Proceedings of the Royal Society B: Biological Sciences* **282**, 20151075 (2015).
12. C. E. Tarnita, C. H. Taubes, M. A. Nowak, Evolutionary construction by staying together and coming together. *Journal of Theoretical Biology* **320**, 10–22 (2013).
13. J. T. Bonner, Aggregation and Differentiation in the Cellular Slime Molds. *Annual Review of Microbiology* **25**, 75–92 (1971).
14. E. F. Keller, L. A. Segel, Initiation of slime mold aggregation viewed as an instability. *Journal of Theoretical Biology* **26**, 399–415 (1970).
15. M. D. Herron, J. M. Borin, J. C. Boswell, J. Walker, I.-C. K. Chen, C. A. Knox, M. Boyd, F. Rosenzweig, W. C. Ratcliff, De novo origins of multicellularity in response to predation. *Sci Rep* **9**, 2328 (2019).
16. R. H. Kessin, G. G. Gundersen, V. Zaydfudim, M. Grimson, How cellular slime molds evade nematodes. *Proceedings of the National Academy of Sciences* **93**, 4857–4861 (1996).
17. T. Trunk, H. S. Khalil, J. C. Leo, Bacterial autoaggregation. *AIMS Microbiol* **4**, 140–164 (2018).
18. M. Stratford, Lectin-mediated Aggregation of Yeasts — Yeast Flocculation. *Biotechnology and Genetic Engineering Reviews* **10**, 283–342 (1992).
19. N. Ros-Rocher, A. Pérez-Posada, M. M. Leger, I. Ruiz-Trillo, The origin of animals: an ancestral reconstruction of the unicellular-to-multicellular transition. *Open Biology* **11**, 200359 (2021).
20. D. S. Booth, N. King, "The history of Salpingoeca rosetta as a model for reconstructing animal origins" in *Current Topics in Developmental Biology* (Elsevier, 2022; https://linkinghub.elsevier.com/retrieve/pii/S0070215322000011)vol. 147, pp. 73–91.
21. N. Ros-Rocher, T. Brunet, What is it like to be a choanoflagellate? Sensation, processing and behavior in the closest unicellular relatives of animals. *Anim Cogn* **26**, 1767–1782 (2023).
22. M. Carr, B. S. C. Leadbeater, R. Hassan, M. Nelson, S. L. Baldauf, Molecular phylogeny of choanoflagellates, the sister group to Metazoa. *Proc. Natl. Acad. Sci. U.S.A.* **105**, 16641–16646 (2008).
23. B. S. C. Leadbeater, *The Choanoflagellates: Evolution, Biology and Ecology* (Cambridge University Press, Cambridge, 2015; https://www.cambridge.org/core/books/choanoflagellates/675095F5862C46DFA91EBB57E4CD65C2).
24. S. R. Fairclough, M. J. Dayel, N. King, Multicellular development in a choanoflagellate. *Current Biology* **20**, R875–R876 (2010).
25. S. R. Fairclough, Z. Chen, E. Kramer, Q. Zeng, S. Young, H. M. Robertson, E. Begovic, D. J. Richter, C. Russ, M. J. Westbrook, G. Manning, B. F. Lang, B. Haas, C. Nusbaum, N. King, Premetazoan genome evolution and the regulation of cell differentiation in the choanoflagellate Salpingoeca rosetta. *Genome Biology* **14**, R15 (2013).
26. M. J. Dayel, R. A. Alegado, S. R. Fairclough, T. C. Levin, S. A. Nichols, K. McDonald, N. King, Cell differentiation and morphogenesis in the colony-forming choanoflagellate *Salpingoeca rosetta*. *Developmental Biology* **357**, 73–82 (2011).
27. E. Hehenberger, D. V. Tikhonenkov, M. Kolisko, J. Del Campo, A. S. Esaulov, A. P. Mylnikov, P. J. Keeling, Novel Predators Reshape Holozoan Phylogeny and Reveal the Presence of a Two-Component Signaling System in the Ancestor of Animals. *Curr Biol* **27**, 2043-2050.e6 (2017).
28. A. Sebé-Pedrós, M. Irimia, J. del Campo, H. Parra-Acero, C. Russ, C. Nusbaum, B. J. Blencowe, I. Ruiz-Trillo, Regulated aggregative multicellularity in a close unicellular relative of metazoa. *eLife* **2**, e01287 (2013).
29. A. P. Mylnikov, D. V. Tikhonenkov, S. A. Karpov, C. Wylezich, Microscopical Studies on *Ministeria vibrans* Tong, 1997 (Filasterea) Highlight the Cytoskeletal Structure of the Common Ancestor of Filasterea, Metazoa and Choanoflagellata. *Protist* **170**, 385–396 (2019).
30. D. V. Tikhonenkov, K. V. Mikhailov, E. Hehenberger, S. A. Karpov, K. I. Prokina, A. S. Esaulov, O. I. Belyakova, Y. A. Mazei, A. P. Mylnikov, V. V. Aleoshin, P. J. Keeling, New Lineage of Microbial Predators Adds Complexity to Reconstructing the Evolutionary Origin of Animals. *Current Biology* **30**, 4500-4509.e5 (2020).
31. Q. Du, Y. Kawabe, C. Schilde, Z. Chen, P. Schaap, The Evolution of Aggregative Multicellularity and Cell–Cell Communication in the Dictyostelia. *Journal of Molecular Biology* **427**, 3722–3733 (2015).
32. E. Haeckel, E. P. Wright F. L. S., Memoirs: The Gastraea-Theory, the Phylogenetic Classification of the Animal Kingdom and the Homology of the Germ-Lamellæ. *Journal of Cell Science* **s2-14**, 223–247 (1874).
33. C. Nielsen, Six major steps in animal evolution: are we derived sponge larvae? *Evol Dev* **10**, 241–257 (2008).
34. D. Arendt, E. Benito-Gutierrez, T. Brunet, H. Marlow, Gastric pouches and the mucociliary sole: setting the stage for nervous system evolution. *Philosophical Transactions of the Royal Society B: Biological Sciences* **370**, 20150286 (2015).

35. T. Brunet, B. T. Larson, T. A. Linden, M. J. A. Vermeij, K. McDonald, N. King, Light-regulated collective contractility in a multicellular choanoflagellate. *Science* **366**, 326–334 (2019).
36. T. Brunet, D. S. Booth, "Cell polarity in the protist-to-animal transition" in *Current Topics in Developmental Biology* (Elsevier, 2023; https://linkinghub.elsevier.com/retrieve/pii/S0070215323000455), p. S0070215323000455.
37. J. Reyes-Rivera, Y. Wu, B. G. H. Guthrie, M. A. Marletta, N. King, T. Brunet, Nitric oxide signaling controls collective contractions in a colonial choanoflagellate. *Current Biology* **32**, 2539-2547.e5 (2022).
38. E. Ocaña-Pallarès, T. A. Williams, D. López-Escardó, A. S. Arroyo, J. S. Pathmanathan, E. Bapteste, D. V. Tikhonenkov, P. J. Keeling, G. J. Szöllősi, I. Ruiz-Trillo, Divergent genomic trajectories predate the origin of animals and fungi. *Nature* **609**, 747–753 (2022).
39. X. Grau-Bové, G. Torruella, S. Donachie, H. Suga, G. Leonard, T. A. Richards, I. Ruiz-Trillo, Dynamics of genomic innovation in the unicellular ancestry of animals. *Elife* **6**, e26036 (2017).
40. N. King, M. J. Westbrook, S. L. Young, A. Kuo, M. Abedin, J. Chapman, S. Fairclough, U. Hellsten, Y. Isogai, I. Letunic, M. Marr, D. Pincus, N. Putnam, A. Rokas, K. J. Wright, R. Zuzow, W. Dirks, M. Good, D. Goodstein, D. Lemons, W. Li, J. B. Lyons, A. Morris, S. Nichols, D. J. Richter, A. Salamov, J. G. I. Sequencing, P. Bork, W. A. Lim, G. Manning, W. T. Miller, W. McGinnis, H. Shapiro, R. Tjian, I. V. Grigoriev, D. Rokhsar, The genome of the choanoflagellate Monosiga brevicollis and the origin of metazoans. *Nature* **451**, 783–788 (2008).
41. G. Torruella, A. de Mendoza, X. Grau-Bové, M. Antó, M. A. Chaplin, J. del Campo, L. Eme, G. Pérez-Cordón, C. M. Whipps, K. M. Nichols, R. Paley, A. J. Roger, A. Sitjà-Bobadilla, S. Donachie, I. Ruiz-Trillo, Phylogenomics Reveals Convergent Evolution of Lifestyles in Close Relatives of Animals and Fungi. *Curr Biol* **25**, 2404–2410 (2015).
42. N. Ros-Rocher, R. Q. Kidner, C. Gerdt, W. S. Davidson, I. Ruiz-Trillo, J. P. Gerdt, Chemical factors induce aggregative multicellularity in a close unicellular relative of animals. *Proc. Natl. Acad. Sci. U.S.A.* **120**, e2216668120 (2023).
43. B. Kjerfve, CARICOMP: Caribbean coral reef, seagrass and mangrove sites. (1998).
44. B. S. Leadbeater, Life-history and ultrastructure of a new marine species of Proterospongia (Choanoflagellida). *Journal of the Marine Biological Association of the United Kingdom* **63**, 135–160 (1983).
45. C. Little, J. A. Kitching, *The Biology of Rocky Shores* (Oxford University Press, 1996).
46. D. Garbary, "The Margin of the Sea" in *Algae and Cyanobacteria in Extreme Environments*, J. Seckbach, Ed. (Springer Netherlands, Dordrecht, 2007; https://doi.org/10.1007/978-1-4020-6112-7_9)*Cellular Origin, Life in Extreme Habitats and Astrobiology*, pp. 173–191.
47. J. Huggett, C. Griffiths, Some relationships between elevation, physico-chemical variables and biota of intertidal rock pools. *Mar. Ecol. Prog. Ser.* **29**, 189–197 (1986).
48. E. Amsalem, G. Rilov, High thermal plasticity, and vulnerability, in extreme environments at the warm distributional edge: The case of a tidepool shrimp. *Journal of Experimental Marine Biology and Ecology* **545**, 151641 (2021).
49. I. R. Davison, G. A. Pearson, Stress Tolerance in Intertidal Seaweeds. *Journal of Phycology* **32**, 197–211 (1996).
50. F. Stein, *Der Organismus Der Infusionsthiere* (W. Engelmann, Leipzig, 1859; https://www.biodiversitylibrary.org/bibliography/3933).
51. W. Saville-Kent, *A Manual of the Infusoria : Including a Description of All Known Flagellate, Ciliate, and Tentaculiferous Protozoa, British and Foreign, and an Account of the Organization and the Affinities of the Sponges* (D. Bogue, London, 1880; https://www.biodiversitylibrary.org/bibliography/10143).
52. M. Reess, C. Fisch, *Untersuchungen über bau und Lebensgeschichte der Hirschtrüffel, Elaphomyces* (T. Fischer, 1887).
53. B. S. C. Leadbeater, S. A. Karpov, Cyst Formation in a Freshwater Strain of the Choanoflagellate Desmarella moniliformis Kent. *Journal of Eukaryotic Microbiology* **47**, 433–439 (2000).
54. D. Stoupin, A. K. Kiss, H. Arndt, A. V. Shatilovich, D. A. Gilichinsky, F. Nitsche, Cryptic diversity within the choanoflagellate morphospecies complex *Codosiga botrytis* – Phylogeny and morphology of ancient and modern isolates. *European Journal of Protistology* **48**, 263–273 (2012).
55. A. Jeuck, H. Arndt, F. Nitsche, Extended phylogeny of the Craspedida (Choanomonada). *European Journal of Protistology* **50**, 430–443 (2014).
56. P. C. Venter, F. Nitsche, H. Arndt, The Hidden Diversity of Flagellated Protists in Soil. *Protist* **169**, 432–449 (2018).
57. J. D. van Elsas, J. T. Trevors, A. S. Rosado, P. Nannipieri, *Modern Soil Microbiology, Third Edition* (CRC Press, 2019).
58. T. Brunet, M. Albert, W. Roman, M. C. Coyle, D. C. Spitzer, N. King, A flagellate-to-amoeboid switch in the closest living relatives of animals. *eLife* **10**, e61037 (2021).
59. Y. Li, Y. Wang, S. Zhang, X. X. Maurer-Alcalá, Y. Yan, How Ciliated Protists Survive by Cysts: Some Key Points During Encystment and Excystment. *Frontiers in Microbiology* **13** (2022).
60. P. Schaap, C. Schilde, Encystation: the most prevalent and underinvestigated differentiation pathway of eukaryotes. *Microbiology* **164**, 727–739 (2018).
61. F. Verni, G. Rosati, Resting cysts: A survival strategy in Protozoa Ciliophora. *Italian Journal of Zoology* **78**, 134–145 (2011).
62. A. J. Griffiths, "Encystment in Amoebae" in *Advances in Microbial Physiology*, A. H. Rose, J. F. Wilkinson, Eds. (Academic Press, 1969; https://www.sciencedirect.com/science/article/pii/S0065291108604403)vol. 4, pp. 105–129.
63. Z.-W. Gong, X.-P. Fan, R. Ma, B. Ni, Ultrastructure of vegetative cells and resting cysts, and live observations of the encystation and excystation processes in Diophrys oligothrix Borror, 1965 (Protista, Ciliophora). *Journal of Morphology* **279**, 1397–1407 (2018).
64. B. Bowers, E. D. Korn, THE FINE STRUCTURE OF ACANTHAMOEBA CASTELLANII (NEFF STRAIN) : II. Encystment. *Journal of Cell Biology* **41**, 786–805 (1969).
65. J. O. Corliss, S. C. Esser, Comments on the Role of the Cyst in the Life Cycle and Survival of Free-Living Protozoa. *Transactions of the American Microscopical Society* **93**, 578–593 (1974).
66. F. Chen, Y. Xue, N. Pan, M. Z. Bhatti, T. Niu, J. Chen, New contribution to the morphology and molecular mechanism of Euplotes encysticus encystment. *Sci Rep* **8**, 12795 (2018).
67. G. W. Grimes, Differentiation During Encystment and Excystment in Oxytricha fallax*. *The Journal of Protozoology* **20**, 92–104 (1973).
68. M. S. Atkins, O. R. Anderson, C. O. Wirsen, Effect of hydrostatic pressure on the growth rates and encystment of flagellated protozoa isolated from a deep-sea hydrothermal vent and a deep shelf region. *Marine Ecology Progress Series* **171**, 85–95 (1998).

69. N. A. Khan, J. Iqbal, R. Siddiqui, Stress Management in Cyst-Forming Free-Living Protists: Programmed Cell Death and/or Encystment. *BioMed Research International* **2015**, e437534 (2015).
70. C. Di Ciano, Z. Nie, K. Szászi, A. Lewis, T. Uruno, X. Zhan, O. D. Rotstein, A. Mak, A. Kapus, Osmotic stress-induced remodeling of the cortical cytoskeleton. *American Journal of Physiology-Cell Physiology* **283**, C850–C865 (2002).
71. G. Komis, P. Apostolakos, B. Galatis, Hyperosmotic stress-induced actin filament reorganization in leaf cells of Chlorophyton comosum. *Journal of Experimental Botany* **53**, 1699–1710 (2002).
72. F. Rivero, B. Köppel, B. Peracino, S. Bozzaro, F. Siegert, C. J. Weijer, M. Schleicher, R. Albrecht, A. A. Noegel, The role of the cortical cytoskeleton: F-actin crosslinking proteins protect against osmotic stress, ensure cell size, cell shape and motility, and contribute to phagocytosis and development. *Journal of Cell Science* **109**, 2679–2691 (1996).
73. H. Aizawa, M. Katadae, M. Maruya, M. Sameshima, K. Murakami-Murofushi, I. Yahara, Hyperosmotic stress-induced reorganization of actin bundles in Dictyostelium cells over-expressing cofilin. *Genes to Cells* **4**, 311–324 (1999).
74. S. Balachandra, S. Sarkar, A. A. Amodeo, The Nuclear-to-Cytoplasmic Ratio: Coupling DNA Content to Cell Size, Cell Cycle, and Biosynthetic Capacity. *Annu Rev Genet* **56**, 165–185 (2022).
75. T. Fenchel, Filter-feeding in Colonial Protists. *Protist* **170**, 283–286 (2019).
76. M. a. R. Koehl, Selective factors in the evolution of multicellularity in choanoflagellates. *Journal of Experimental Zoology Part B: Molecular and Developmental Evolution* **336**, 315–326 (2021).
77. T. Cavalier-Smith, Origin of animal multicellularity: precursors, causes, consequences—the choanoflagellate/sponge transition, neurogenesis and the Cambrian explosion. *Philosophical Transactions of the Royal Society B: Biological Sciences* **372**, 20150476 (2017).
78. J. B. Kirkegaard, R. E. Goldstein, Filter-feeding, near-field flows, and the morphologies of colonial choanoflagellates. *Phys. Rev. E* **94**, 052401 (2016).
79. N. J. L'Etoile, C. King-Smith, Rosette Colonies of Choanoflagellates (Salpingoeca rosetta) Show Increased Food Vacuole Formation Compared with Single Swimming Cells. *Journal of Eukaryotic Microbiology* **67**, 263–267 (2020).
80. S. M. Stanley, An Ecological Theory for the Sudden Origin of Multicellular Life in the Late Precambrian. *Proceedings of the National Academy of Sciences* **70**, 1486–1489 (1973).
81. K. Tong, G. O. Bozdag, W. C. Ratcliff, Selective drivers of simple multicellularity. *Current Opinion in Microbiology* **67**, 102141 (2022).
82. D. J. Richter, N. King, The Genomic and Cellular Foundations of Animal Origins. *Annual Review of Genetics* **47**, 509–537 (2013).
83. J. B. Kirkegaard, R. E. Goldstein, Filter-feeding, near-field flows, and the morphologies of colonial choanoflagellates. *Phys. Rev. E* **94**, 052401 (2016).
84. M. E. Boraas, D. B. Seale, J. E. Boxhorn, Phagotrophy by a flagellate selects for colonial prey: A possible origin of multicellularity. *Evolutionary Ecology* **12**, 153–164 (1998).
85. N. E. Chin, T. C. Wu, J. M. O'Toole, K. Xu, T. Hata, M. A. R. Koehl, Formation of multicellular colonies by choanoflagellates increases susceptibility to capture by amoeboid predators. *Journal of Eukaryotic Microbiology* **70**, e12961 (2023).
86. W. E. Kumler, J. Jorge, P. M. Kim, N. Iftekhar, M. a. R. Koehl, Does Formation of Multicellular Colonies by Choanoflagellates Affect Their Susceptibility to Capture by Passive Protozoan Predators? *Journal of Eukaryotic Microbiology* **67**, 555–565 (2020).
87. M. Roper, M. J. Dayel, R. E. Pepper, M. a. R. Koehl, Cooperatively generated stresslet flows supply fresh fluid to multicellular choanoflagellate colonies. *Phys. Rev. Lett.* **110**, 228104 (2013).
88. M. B. Short, C. A. Solari, S. Ganguly, T. R. Powers, J. O. Kessler, R. E. Goldstein, Flows driven by flagella of multicellular organisms enhance long-range molecular transport. *Proceedings of the National Academy of Sciences* **103**, 8315–8319 (2006).
89. S. Tang, Y. Pichugin, K. Hammerschmidt, An environmentally induced multicellular life cycle of a unicellular cyanobacterium. *Current Biology* **33**, 764-769.e5 (2023).
90. K. Mizuno, M. Maree, T. Nagamura, A. Koga, S. Hirayama, S. Furukawa, K. Tanaka, K. Morikawa, Novel multicellular prokaryote discovered next to an underground stream. *eLife* **11**, e71920 (2022).
91. J. Barrere, P. Nanda, A. W. Murray, Alternating selection for dispersal and multicellularity favors regulated life cycles. *Current Biology* **33**, 1809-1817.e3 (2023).
92. Y. Pichugin, H. J. Park, A. Traulsen, Evolution of simple multicellular life cycles in dynamic environments. *J. R. Soc. Interface.* **16**, 20190054 (2019).
93. M. Staps, J. Van Gestel, C. E. Tarnita, "Life Cycles as a Central Organizing Theme for Studying Multicellularity" in *The Evolution of Multicellularity* (CRC Press, 2022).
94. H. James-Clark A. B., IV.—Conclusive proofs of the animality of the ciliate sponges, and of their affinities with the Infusoria flagellata. *Annals and Magazine of Natural History*, doi: 10.1080/00222936708679703 (1867).
95. K. S.a, C. S.j, A revision of choanoflagellate genera Kentrosiga Schiller, 1953 and Desmarella Kent, 1880. *Acta Protozoologica* **1** (1998).
96. B. S. C. Leadbeater, Life-history and ultrastructure of a new marine species of Proterospongia (Choanoflagellida). *Journal of the Marine Biological Association of the United Kingdom* **63**, 135–160 (1983).
97. D. J. Hibberd, Observations on the ultrastructure of the choanoflagellate Codosiga botrytis (Ehr.) saville-kent with special reference to the flagellar apparatus. *Journal of Cell Science* **17**, 191–219 (1975).
98. M. E. Pettitt, B. A. A. Orme, J. R. Blake, B. S. C. Leadbeater, The hydrodynamics of filter feeding in choanoflagellates. *European Journal of Protistology* **38**, 313 (2002).
99. W. L. Marshall, M. L. Berbee, Facing Unknowns: Living Cultures (*Pirum gemmata* gen. nov., sp. nov., and *Abeoforma whisleri*, gen. nov., sp. nov.) from Invertebrate Digestive Tracts Represent an Undescribed Clade within the Unicellular Opisthokont Lineage Ichthyosporea (Mesomycetozoea). *Protist* **162**, 33–57 (2011).
100. H. Suga, I. Ruiz-Trillo, Development of ichthyosporeans sheds light on the origin of metazoan multicellularity. *Developmental Biology* **377**, 284–292 (2013).
101. A. de Mendoza, H. Suga, J. Permanyer, M. Irimia, I. Ruiz-Trillo, Complex transcriptional regulation and independent evolution of fungal-like traits in a relative of animals. *eLife* **4**, e08904 (2015).
102. O. Dudin, A. Ondracka, X. Grau-Bové, A. A. Haraldsen, A. Toyoda, H. Suga, J. Bråte, I. Ruiz-Trillo, A unicellular relative of animals generates a layer of polarized cells by actomyosin-dependent cellularization. *eLife* **8**, e49801 (2019).

103. A. Kożyczkowska, S. R. Najle, E. Ocaña-Pallarès, C. Aresté, V. Shabardina, P. S. Ara, I. Ruiz-Trillo, E. Casacuberta, Stable transfection in protist *Corallochytrium limacisporum* identifies novel cellular features among unicellular animals relatives. *Current Biology* **31**, 4104-4110.e5 (2021).

104. H. Shah, M. Olivetta, C. Bhickta, P. Ronchi, M. Trupinić, E. C. Tromer, I. M. Tolić, Y. Schwab, O. Dudin, G. Dey, "Life cycle-coupled evolution of mitosis in close relatives of animals" (preprint, Cell Biology, 2023); https://doi.org/10.1101/2023.05.10.540163.

105. L. G. Nagy, T. Varga, Á. Csernetics, M. Virágh, Fungi took a unique evolutionary route to multicellularity: Seven key challenges for fungal multicellular life. *Fungal Biology Reviews* **34**, 151–169 (2020).

106. M. W. Brown, F. W. Spiegel, J. D. Silberman, Phylogeny of the "forgotten" cellular slime mold, Fonticula alba, reveals a key evolutionary branch within Opisthokonta. *Mol Biol Evol* **26**, 2699–2709 (2009).

107. C. Toret, A. Picco, M. Boiero-Sanders, A. Michelot, M. Kaksonen, The cellular slime mold *Fonticula alba* forms a dynamic, multicellular collective while feeding on bacteria. *Current Biology* **32**, 1961-1973.e4 (2022).

108. K. Sauer, P. Stoodley, D. M. Goeres, L. Hall-Stoodley, M. Burmølle, P. S. Stewart, T. Bjarnsholt, The biofilm life cycle: expanding the conceptual model of biofilm formation. *Nat Rev Microbiol* **20**, 608–620 (2022).

109. Q. Du, Y. Kawabe, C. Schilde, Z.-H. Chen, P. Schaap, The Evolution of Aggregative Multicellularity and Cell-Cell Communication in the Dictyostelia. *J. Mol. Biol.* **427**, 3722–3733 (2015).

110. M. W. Brown, J. D. Silberman, "The Non-dictyostelid Sorocarpic Amoebae" in *Dictyostelids*, M. Romeralo, S. Baldauf, R. Escalante, Eds. (Springer Berlin Heidelberg, Berlin, Heidelberg, 2013; http://link.springer.com/10.1007/978-3-642-38487-5_12), pp. 219–242.

111. M. W. Brown, M. Kolisko, J. D. Silberman, A. J. Roger, Aggregative multicellularity evolved independently in the eukaryotic supergroup Rhizaria. *Curr Biol* **22**, 1123–1127 (2012).

112. P. D. Curtis, R. G. Taylor, R. D. Welch, L. J. Shimkets, Spatial Organization of Myxococcus xanthus during Fruiting Body Formation. *J Bacteriol* **189**, 9126–9130 (2007).

113. J. T. Pentz, K. MacGillivray, J. G. DuBose, P. L. Conlin, E. Reinhardt, E. Libby, W. C. Ratcliff, Evolutionary consequences of nascent multicellular life cycles. *eLife* **12**, e84336 (2023).

114. K. Hammerschmidt, C. J. Rose, B. Kerr, P. B. Rainey, Life cycles, fitness decoupling and the evolution of multicellularity. *Nature* **515**, 75–79 (2014).

115. R. E. Michod, Evolution of individuality during the transition from unicellular to multicellular life. *Proc. Natl. Acad. Sci. U.S.A.* **104 Suppl 1**, 8613–8618 (2007).

116. J. E. Strassmann, Y. Zhu, D. C. Queller, Altruism and social cheating in the social amoeba Dictyostelium discoideum. *Nature* **408**, 965–967 (2000).

117. G. J. Velicer, L. Kroos, R. E. Lenski, Developmental cheating in the social bacterium Myxococcus xanthus. *Nature* **404**, 598–601 (2000).

118. D. C. Queller, E. Ponte, S. Bozzaro, J. E. Strassmann, Single-Gene Greenbeard Effects in the Social Amoeba Dictyostelium discoideum. *Science* **299**, 105–106 (2003).

119. N. Gruenheit, K. Parkinson, B. Stewart, J. A. Howie, J. B. Wolf, C. R. L. Thompson, A polychromatic 'greenbeard' locus determines patterns of cooperation in a social amoeba. *Nat Commun* **8**, 14171 (2017).

120. R. Benabentos, S. Hirose, R. Sucgang, T. Curk, M. Katoh, E. A. Ostrowski, J. E. Strassmann, D. C. Queller, B. Zupan, G. Shaulsky, A. Kuspa, Polymorphic Members of the lag Gene Family Mediate Kin Discrimination in Dictyostelium. *Current Biology* **19**, 567–572 (2009).

121. S. I. Li, M. D. Purugganan, The cooperative amoeba: Dictyostelium as a model for social evolution. *Trends in Genetics* **27**, 48–54 (2011).

122. A. Espinosa, G. Paz-y-Miño-C, Evidence of taxa-, clone-, and kin-discrimination in protists: ecological and evolutionary implications. *Evol Ecol* **28**, 1019–1029 (2014).

123. J. Smith, J. E. Strassmann, D. C. Queller, Fine-scale spatial ecology drives kin selection relatedness among cooperating amoebae. *Evolution* **70**, 848–859 (2016).

124. S. A. West, A. S. Griffin, A. Gardner, Social semantics: altruism, cooperation, mutualism, strong reciprocity and group selection. *J of Evolutionary Biology* **20**, 415–432 (2007).

125. C. R. Haag, M. Riek, J. W. Hottinger, V. I. Pajunen, D. Ebert, Founder events as determinants of within-island and among-island genetic structure of Daphnia metapopulations. *Heredity* **96**, 150–158 (2006).

126. A. J. Black, P. Bourrat, P. B. Rainey, Ecological scaffolding and the evolution of individuality. *Nat Ecol Evol* **4**, 426–436 (2020).

127. T. Brunet, N. King, "The Single-Celled Ancestors of Animals: A History of Hypotheses" in *The Evolution of Multicellularity* (CRC Press, ed. 1st, 2022; https://www.preprints.org/manuscript/202011.0302/v1).

128. M. Ferrer-Bonet, I. Ruiz-Trillo, Capsaspora owczarzaki. *Current Biology* **27**, R829–R830 (2017).

129. C. Broersma, E. A. Ostrowski, "Group Transformation: Fruiting Body and Stalk Formation" in *The Evolution of Multicellularity* (CRC Press, 2022).

130. S. M. Adl, D. Bass, C. E. Lane, J. Lukeš, C. L. Schoch, A. Smirnov, S. Agatha, C. Berney, M. W. Brown, F. Burki, P. Cárdenas, I. Čepička, L. Chistyakova, J. del Campo, M. Dunthorn, B. Edvardsen, Y. Eglit, L. Guillou, V. Hampl, A. A. Heiss, M. Hoppenrath, T. Y. James, A. Karnkowska, S. Karpov, E. Kim, M. Kolisko, A. Kudryavtsev, D. J. G. Lahr, E. Lara, L. Le Gall, D. H. Lynn, D. G. Mann, R. Massana, E. A. D. Mitchell, C. Morrow, J. S. Park, J. W. Pawlowski, M. J. Powell, D. J. Richter, S. Rueckert, L. Shadwick, S. Shimano, F. W. Spiegel, G. Torruella, N. Youssef, V. Zlatogursky, Q. Zhang, Revisions to the Classification, Nomenclature, and Diversity of Eukaryotes. *Journal of Eukaryotic Microbiology* **66**, 4–119 (2019).